Fibers and Polymers 2020, Vol.21, No.8, 1694-1703
DOI 10.1007/s12221-020-9922-8

ISSN 1229-9197 (print version)
ISSN 1875-0052 (electronic version)

Fabrication and Characterization of Electrospun Scaffold Based on Polycaprolactone-Aloe vera and Polyvinyl Alcohol for Skin Tissue Engineering

Marjan Shabannejad[1], Mohammad Sadegh Nourbakhsh[1,2]*, Amir Salati[3], and Zohreh Bahrami[4]

[1]*Department of Biomedical Engineering, Faculty of New Sciences and Technologies, Semnan University, Semnan 3513119111, Iran*
[2]*Faculty of Materials and Metallurgical Engineering, Semnan University, Semnan 3513119111, Iran*
[3]*Nervous System Stem Cells Research Center, Semnan University of Medical Sciences, Semnan 3514799442, Iran*
[4]*Nanochemistry Group, Faculty of New Sciences and Technologies, Semnan University, Semnan 3513119111, Iran*
(Received September 5, 2019; Revised November 30, 2019; Accepted December 6, 2019)

Abstract: In the present work, the biodegradable nanofibrous scaffolds containing poly(caprolactone) (PCL), poly(vinyl alcohol) (PVA) and aloe vera (AV), through two nozzles electrospinning method, were prepared and characterized by scanning electron microscopy, Fourier transform infrared spectroscopy, contact angle measurement and mechanical analysis. The biocompatibility and cell growth were evaluated using MTT (3-(4, 5-dimethylthiazol-2-yl)-2, 5-diphenyltetrazolium bromide) assay. Adding poly(vinyl alcohol) (PVA) and poly(caprolactone) (PCL) boosted the electrospinability of aloe vera (AV) solution and mechanical features of the scaffolds. According to the Scanning electron microscopy (SEM) results, uniform PVA/AV-PCL nanofibers were fabricated with the average diameter about 119±11.78 nm. Fourier-transform infrared spectroscopy) FTIR (confirmed the presence of functional groups of scaffolds. The results of the contact angle showed that by adding aloe vera, the hydrophilicity increased. The results showed that the tensile strength of samples with 6 mg/m*l* AV, reached to 2.02 MPa. MTT results showed that all samples had a cell viability of over 80 %. It can be concluded that nanofibrous scaffolds with concentration of 6 mg/m*l*, distance between syringe tip/collector of 15 cm, feed rate of 3 m*l*/h and applied voltage of 12 kV, have appropriate properties for skin tissue engineering by stimulating the fibroblast cells and therefore accelerating the regeneration processes of damaged skin.

Keywords: Electrospinning, Aloe vera, Poly(caprolactone), Poly(vinyl alcohol), Tissue engineering

Introduction

Skin has numerous functions including regulation of temperature, guiding physical senses and mechanical barrier to protect the body against microorganisms, and harmful environmental factors such as radiation, mechanical injuries, heat and chemical burnings [1,2]. For artificial skin fabrication, it is necessary to have a suitable substrate as the scaffold for supporting cells. There are many fabrication techniques; among them, electrospinning is the most widely used. At present, numerous methods have been reported for improving the production rate of fibers using electrospinning, with the group of such methods being led by the multi-nozzle electrospinning. In this method, multiple jets of a polymeric fluid are simultaneously flown through multiple nozzles. This technique not only improves the electrospinning rate, but also provides concurrent electrospinning of polymeric fibers [3-7]. Several factors can affect the fiber diameter and uniformity of electrospun mat. These factors are the structure and properties of the polymer substance (chemical structure, molecular weight, stereo-configuration of the polymer chain), properties of electrospinning solution (solution concentration, viscosity, surface tension, conductivity, solvent volatility and temperature), process condition (voltage, nozzle-collector distance, feeding rate and shape of the collector) and environmental factors (humidity and pressure) [8-16]. Nanofibers have been produced by applying various natural and synthetic polymers. Polycaprolactone is a semi-crystalline, hydrophobic, and non-toxic polymer with excellent mechanical properties, good biocompatibility, low antigenicity, simple processability, and low melting point. Owing to its flexible structure, polycaprolactone can be used to improve the elasticity of rubbers. It can be also employed for medical purposes due to its biocompatibility and low biodegradability [17]. Poly(vinyl alcohol) is a biodegradable water-soluble synthetic polymer possessing high tensile strength and flexibility and great resistance against gas penetration [18]. Aloe vera is a cactus-like and succulent plant with high water content whose leaves contain mucilage tissues. These mucilage tissues have glycoproteins and can prevent inflammation and pain; hence, they can enhance the recovery procedure. This plant also contains polysaccharides, which can stimulate cell proliferation by influencing the fibroblast growth receptors. The aloe vera not only increases the level of collagen only locally near the wounds, but also it restructures the collagen to boost the development of cross-links at the wound and hence facilitating the wound closure [19-25]. Many researchers reported nanofibrous scaffolds with aloe vera for skin tissue engineering. Aloe vera incorporated with PVA membrane displayed hydrophilicity, suitable mechanical strength, degradation, wettability, antibacterial, mechanical strength properties and cell

*Corresponding author: s_nourbakhsh@semnan.ac.ir

compatibility with fibroblasts. The results demonstrated that PVA/AV hydrogel film could be suggested for improving wound treatment [26]. Aloe vera- PVA nanofibrous scaffold can be used as an aloe vera release system in wound care, too. In the first hour, at least 60 % of aloe vera is released and about 90 % of aloe vera is released within 2-4 hours depending on the diameter of the nanofibrous scaffolds [27]. Aloe vera/PCL membranes with ratios from 100/00 to 70/30 showed integration of nanofibers diameter and suitable mechanical features of the scaffolds [28]. In a study, nanofibrous scaffold including aloe vera/PCL was fabricated through electrospinning. Finally, its biological characteristics like biodegradability, cell compatibility, mechanical and chemical characteristics of the scaffolds were characterized. Since aloe vera cannot be electrospun alone properly for the production of nanofibers, an auxiliary biopolymer with desired properties is used for fabrication of scaffolds [29]. In another study, nanofibrous scaffolds were fabricated from Gel/AV/PCL blend by applying double nozzle electrospinning process. RSM method was applied to optimize the electrospinning parameters. The results showed that the presence of AV in this electrospun scaffold improved the cell fibroblast proliferation in comparison with PCL and Gel-PCL [30]. Zarekhalili *et al.* assessed the mechanical, morphological and biological features of polycaprolactone/poly(vinyl alcohol)/gum tragacanth nanofibers produced by electrospinning. They achieved nanofibers with suitable morphology and diameters in the range of 131±27 nm. In addition, MTT ((3-(4,5-dimethylthiazol-2-yl)-2,5-diphenyltetrazolium bromide) assay results indicated no toxicity and proliferation of the fibroblast cells [31].

Recently, the application of statistical methods for designing the experiments has attracted considerable attention in science and engineering researches. Different methods of the design of experiment such as Taguchi, response surface methodology (RSM), artificial neural network (ANN), group method of data handling (GMDH) etc., were used to improve and optimize the electrospinning conditions. These ready-to-use methods (compared to the conventional methods) are beneficial in terms of high precision, lower number of experiments, shorter time and lower costs [32-35].

Nevertheless, applying AV (aloe vera) incorporated to PCL (polycaprolactone) and PVA (polyvinyl alcohol) for fabricating nanofibrous scaffolds for skin tissue engineering have not been reported. The purpose of this study is fabrication and characterization of electrospun scaffold based on polycaprolactone-aloe vera and polyvinyl alcohol for skin tissue engineering.

The most significant competitive advantage of this plant is the use of aloe vera, as a medicinal herb, to replace expensive drugs that are often associated with irreversible side effects. Hence, the main aim of the study is to fabricate a novel scaffold based on PVA-PCL combined AV for skin tissue engineering. In this study, we have examined the combined effect of these scaffolds. Further, the hydrophilicity properties, cell compatibility with fibroblasts and mechanical strength were evaluated to validate the scaffolds as an ideal replacement for the remodeling damaged skin tissues.

Experimental

Materials

Aloe vera powder was purchased from TebJooyan Tabiat Bonyan Co (Iran). PCL with molar mass of 80 KDa, and PVA with molar mass of 85 KDa were supplied from Sigma-Aldrich (USA). Dimethylformamid (DMF) and Dichloromethane (DCM) solvents were supplied by Merck Co (Germany).

Electrospinning Process

To prepare PVA solution, 0.08 g of PVA was added to 1 m*l* of water and stirred for 2 h at 40 °C, then the aloe vera powder was added to the PVA solution with different ratios: 1.25 %, 5 %, 7.5 % and stirred for 2 h; then, the solution was cooled to ambient temperature. To prepare PCL solutions, a mixed solvent system of DMF/DCM was prepared by 2/1 volumetric ratio and 0.125 g of PCL was added to 1 m*l* of the mixed solvent and stirred for 3 h; AV/PVA and PCL solutions were electrospun spontaneously and resultant meshes were collected on aluminum rotating cylinder.

Design of Experiments

Taguchi experimental design with four parameters (feed rate, applied voltage, tip/collector distance and aloe vera concentration) was employed in three levels. The variable and levels of experimental designs are summarized in Table 1. The experiment factors were calculated based on equation (1) and the average nanofiber diameter (Yi, nm) was selected as the response [36].

$$SNs = -10\mathrm{Log}\left(\frac{1}{n}\sum_{i=1}^{n} yi^2\right) \quad (1)$$

Characterization

Scanning electron microscopy (SEM) was used to explore the microstructural features of nanofibers such as morphology, uniformity, and fiber diameter. Samples were cropped to 1 cm×1 cm and coated with silver. Samples were imaged

Table 1. Variables and levels for experiment design

	Unit	Factors level		
		1	2	3
A. AV concentration	mg/m*l*	1	4	6
B. Feed rate	m*l*/h	1	2	3
C. Voltage	kV	12	18	24
D. Distance	cm	5	10	15

with a voltage of 20 kV using SEM (SEM-Philips x130, USA). Image analysis software (Image J, National Institute of Health, Bethesda, Maryland, USA) was used to determine the average diameter of nanofibers. Hydrophilic behaviors of the samples were evaluated through measuring contact angle and interfacial tension using pendant drop (IFT measurement Apparatus CA-ES10). The contact angle was determined as the average of at least three measurements. Fourier transform infrared spectroscopy (FTIR) analysis was used to examine the functional groups of AV powder, PCL, and PVA nanofibers. FTIR analysis was performed by (SHIMADZU 8400, Japan), over a range of 400-4000 cm^{-1}. By differential scanning calorimetry (DSC), the thermal properties of scaffolds were determined. First, 40 mg of material was put in the chamber, the device was heated with a specific heat rate and energy required for heating the sample was recorded. Finally, energy versus temperature was plotted. DSC test was performed using (METTLER TOLEDO, Switzerland). Mechanical strength is one of the most important requirement of electrospun scaffold. Samples were cropped into 1 cm×3 cm and put in a rectangular paperboard frame. Mechanical properties of scaffolds were evaluated using Instron Tensile/Bending/Compression (model Zwick/Roell Z050, Germany) by 50 N load cell under speed of 20 mm/min. Young's modulus (E), tensile stress (σ), tensile strain (ε) of scaffolds were determined based on tensile stress-strain curves.

MTT Test

This assay was conducted using L929 (NCBI C161) fibroblast cells supplied from Pasteur Institute of Iran. Primary function of the fibroblast cells (L929) is the secretion of precursors for extracellular matrix to support the structural integrity of the connective tissue [37].

The cells were first defrozen and then transferred to RPMI-containing culture medium including 10 % FBS. The flasks were then placed in an incubator at the temperature of 37 °C humidity of 90 % and oxygen concentration of 5 %. Direct content method was applied to determine cell toxicity. The samples were first washed by alcohol and then were exposed to UV radiation. Dimethylthiazol diphenyltetrazolium-bromide assay (Sigma USA, MTT) was based on the changes in the yellow color of tetrazolium powder to dark purple insoluble crystals of formazan. This method is one of the common methods utilized for cytotoxicity evaluation.

For this purpose, first 10^4 cells/100 μ*l* of medium was placed on the sterile samples. The cultured cells was poured to each well of the plate, which was then incubated at 37 °C for 4 h until the cells were adhered to the samples. After ensuring the cells adhesion to the samples, 1 m*l* of culture medium was added to each well. After 3 and 7 days, the medium on the cells was removed as much as possible and 400 μ*l* MTT (0.5 mg/m*l*) was added to each well followed by 4 hours of incubation. The solution was then removed and isopropanol was employed to dissolve the purple crystals. The plate was then placed on the shaker for 15 min, so the MTT sediments were completely dissolved. Next, 100 μ*l* of the purple solution of each well was transferred to 96-well plate. ELISA reader (STAT FAX 2100, USA) was then used to determine the concentration of the material dissolved in isopropanol at the wavelength of 570 nm. The wells with higher number of cells showed higher optical density (OD). Therefore, the well containing maximum number of cells can be determined and compared with the control sample by the below equation.

The cell viability on scaffolds was determined by equation (2):

$$\text{Toxicity\%} = \left(\frac{\text{mean OD of sample}}{\text{mean OD of control}}\right) \times 100 \quad (2)$$

viability: 1- toxicity%

Cell Proliferation on the Nanofibrous Scaffold

The cellular adhesion on the scaffolds was evaluated in the third and seventh days. The scaffolds were first sterilized and put in the wells of a 6-well plate. Then, 20000-30000 cells per 100 μ*l* were poured on the samples and incubated for 4-5 hours. After cellular adhesion, a specific amount of culture medium (including 10 % FBS (fetal bovine serum)) was added to each well. After scaffold removal from the medium, they were washed with PBS (phosphate buffered saline) followed by the application of glutaraldehyde (3.5 %) for cellular stabilization. Then, the samples were kept at refrigerator for 2 h. The stabilizing agent was then removed and the samples were washed twice with deionized water and alcohol (50 %, 60 %, 70 %, 80 %, and 96 %).

Results and Discussion

Influence of Electrospinning Parameters on Diameter of Hybrid PVA/AV-PCL Nanofibers

Biodegradable polymer scaffolds were prepared by an electrospinning method. Experiments were performed

Table 2. Experimental design parameters and responses

Run	Factor				Nanofiber diameter (nm)
	AV concentration (mg/m*l*)	Distance (cm)	Feed rate (m*l*/h)	Voltage (kV)	
1	1	10	1	12	651±29.87
2	1	15	2	18	138±13.54
3	1	20	3	24	139±6.24
4	4	15	1	24	177±29.62
5	4	20	2	12	248±6.0
6	4	10	3	18	392±25.11
7	6	20	1	18	246±13.0
8	6	10	2	24	399±26
9	6	15	3	12	119±11.78

according to Table 1 and the average diameter of nanofibers was determined by Image analysis software (Image J) shown in Table 2. The influence of electrospinning parameters including polymer solutions feed rate, tip/collector distance and applied voltage, on the diameter of nanofibers was explored according to the Taguchi L9 orthogonal array experimental design [36]. The signal to noise (S/N) ratio was used in this analysis. Optimal process parameters were determined using the signal to noise (S/N) ratio and according to the 'smaller-the-better' concept [38], the smallest fiber diameter observed was 119±11.78 nm.

As shown in Figure 2(A), the applied voltage of PVA/AV-PCL solution enhanced the signal to noise (S/N) ratio rate, significantly. In Figure 2(B), the signal to noise (S/N) ratio rate was increased by increasing the feed rate of PVA/AV-PCL solution that could be associated with slow formation of PVA/AV nanofibers in comparison with PCL nanofibers. The highest signal to noise (S/N) ratio was observed for the tip/collector distance of 15 cm (C); further increase in this parameter resulted in signal to noise (S/N) ratio drop that could be due to changes in solvent evaporation time. Moreover, signal to noise (S/N) ratio, which was determined in three concentration levels, first decreased and then increased (D). In other words, increasing the concentration from 4 mg/m*l* to 6 mg/m*l* resulted in the lowest fiber diameter. The solution parameters may be altered by biological constituents that leads to the decrease in the nanofiber diameters. Similar effect was reported in fabrication of electrospun scaffold based on garlic/polyurethane for wound dressing applications [39]. However, the diameter was

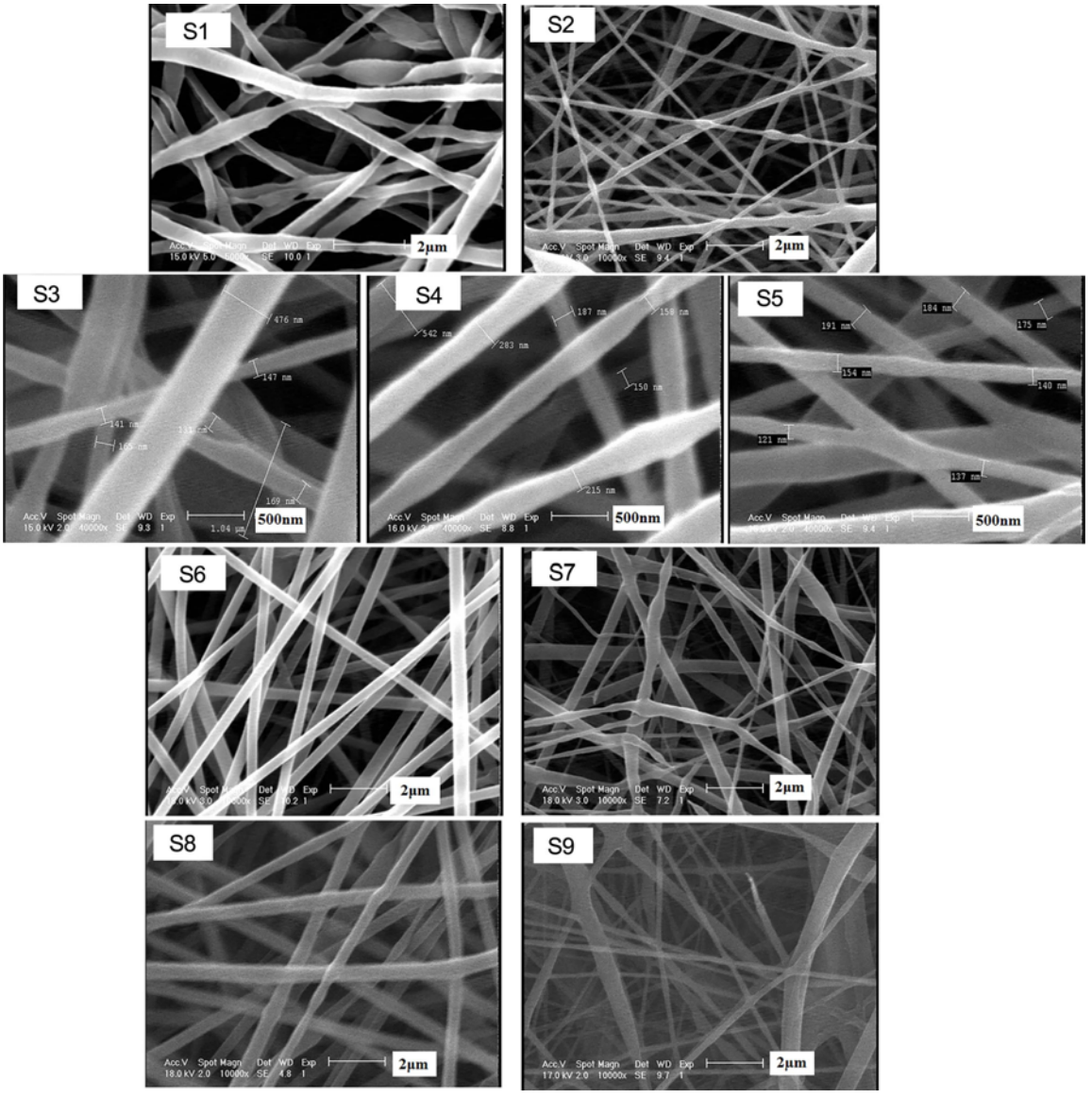

Figure 1. SEM micrographs of electrospun PVA/AV-PCL nanofibers.

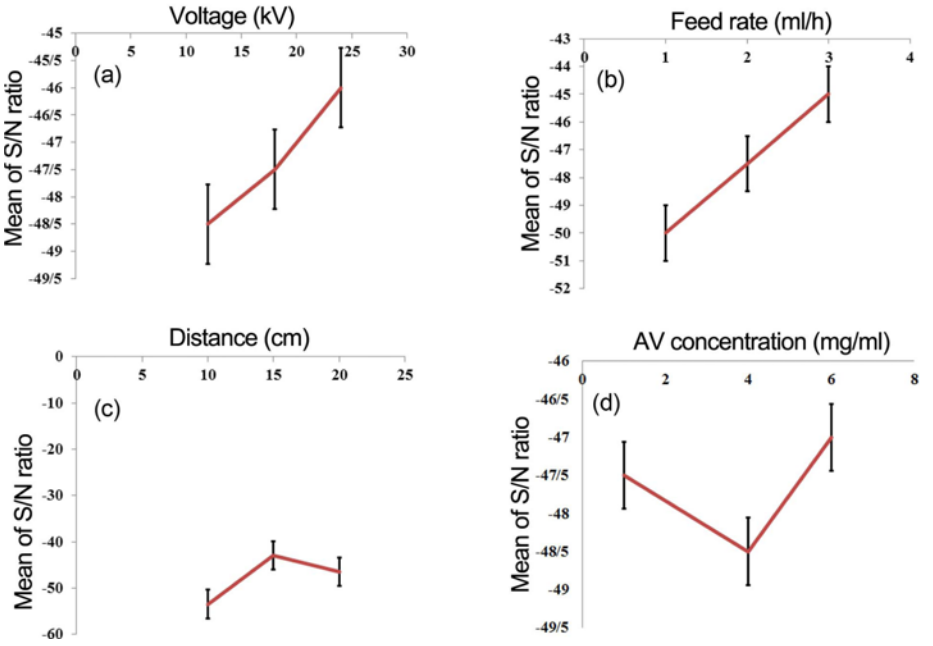

Figure 2. Effect of electrospinning process parameters on nanofiber diameter; (a) applied voltage, (b) feed rate, (c) distance between syringe tip/collector, and (d) aloevera concentration.

increased by increasing the concentration from 1 mg/m*l* to 4 mg/m*l* that could be associated with the increasing the viscosity of the solution that limited the elongation of PVA and AV chains [26].

Nine experimental runs were designed based on Taguchi design for minimizing the diameter of nanofibers (Table 2). Nanofibers with the average diameter of 119±11.78 nm were selected as the optimum scaffolds in which feeding rate, tip-collector distance, applied voltage and aloe vera concentration were 3 m*l*/h, 15 cm, 12 kV and 6 mg/m*l*, respectively.

FTIR

Figure 3 shows the FTIR spectra of PVA/AV-PCL nanofibers. The carbonyl stretching vibrations bands in PCL could be observed at 1728 cm^{-1} and sharp peaks observed at 2929 cm^{-1} and 2864 cm^{-1} in the PCL nanofibers could be attributed to asymmetric and symmetric stretching vibrations of methylene groups, respectively. The bands observed at 1294 cm^{-1}, 1240 cm^{-1} and 1170 cm^{-1} are the distinguishing peaks of PCL associated with the stretching vibrations of C-C and C-O, asymmetric and symmetric stretching vibrations of C-O-C [14]. The sharp peaks observed for pure PVA nanofibers are shown in 2929 cm^{-1} for asymmetric stretching vibrations of methylene groups. The absorption band of PVA at 1047 cm^{-1} matches the stretching vibrations of C-O-C [26].

The peak at 962 cm^{-1} in AV, was due to C-O stretching associated with rhamnogalacturonan side-chain constituent of pectins and the bands appeared at 732 cm^{-1} represents C-H out-of-plane deformation of carbohydrate monomers [40].

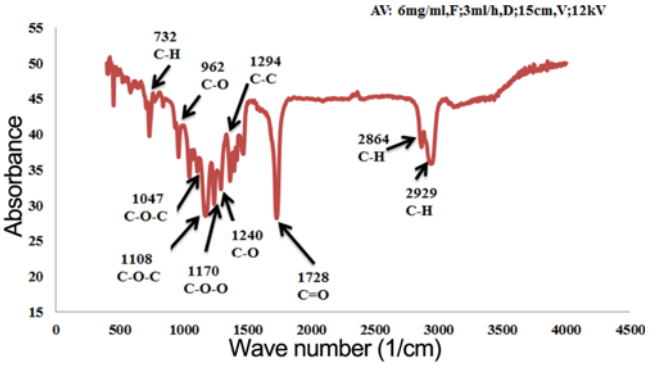

Figure 3. FTIR spectra and PVA/AV-PCL nanofibers.

According to the FTIR results of pure PCL reported by Zarekhalili *et al.*, the peaks at 2946 cm^{-1} and 2864 cm^{-1} were ascribed to the symmetric and asymmetric stretches of CH_2, respectively. While the stretching vibration of carbonyl, C-O and C-C bonds as well as symmetric stretching of C-O-C were shown by the peaks at 1726 cm^{-1}, 1294 cm^{-1} and 1243 cm^{-1}, respectively [31]. According to the FTIR results of pure PVA reported by Mansour *et al.*, the peaks at 1461-1417 cm^{-1} and 2840-3000 cm^{-1} could be assigned to symmetric and asymmetric stretching of CH_2, respectively. The peaks at 1750-1735 cm^{-1}, 1141 cm^{-1} and 1150-1085 cm^{-1} were also associated with the carbonyl, C-O and symmetric stretching of C-O-C, in the respective order [40]. According to FTIR results of aloe vera reported by Rajana *et al.*, the characteristic bonds at 967 cm^{-1} and 708 cm^{-1} are indicative of C-O stretching bond reflecting the presence of rhamnogalacturonan

that is a complex polysaccharide from pectin group. C-H bond also revealed the non-quantum deformation of the carbohydrate monomers, which is in line with the findings of this study [41].

Mechanical Tests

The strength of the electrospun scaffold is dependent on the bulk and architecture mechanical properties of material [42,43]. Figure 4 indicates the stress-strain behaviors of PVA/AV-PCL nanofibrous scaffolds. Elastic modulus, ultimate tensile strength, and fracture strain of electrospun scaffolds are listed in Table 3. Young's modulus, maximum tensile strength, and strain of the nanofibrous scaffolds are 2.02±0.95 MPa, 8.97±2.16 MPa, 74.58±22.79 % respectively. By increasing the concentration of aloe vera and changing electrospinning parameters (feed rates, tip-collector distance, and applied voltages), Young's modulus, tensile strength and tensile strain were increased [27]. Sogania *et al.* fabricated PCL-AV nanofiber scaffold (AV concentrations of 5 % and 10 %) using electrospinning method. Their results indicated that elastic modulus, final yield strength and fracture strain of the electrospun PCL-AV10 % scaffold were higher than PCL-AV5 % scaffold. This means that incorporation of AV into PCL structure enhanced the mechanical properties of the nanofiber scaffold [44]. Furthermore, Carter *et al.* proved that at AV concentrations above 20 %, the tensile strength of the scaffold would decrease due to a decline in bonding affinity of the main functional groups of aloe vera toward other polymers. In general, low contents of AV will enhance the mechanical properties [28].

Certain studies reported that decreased of nanofiber diameter, depends on enhancement of the tensile strength. Mani and Jaganathan observed that fabrication of electrospun scaffold based on PU/grapes reduced fiber and pore diameter that might had increased tensile strength [45]. Also, the electrospun scaffold based on PU/sesame oil and PU/sesame oil/honey/propolis showed enhance the tensile strength of scaffold which could be associated to the reduction of fibers diameter [46] By comparing the obtained results, it can be found that the Young's modulus, the final yield strength and the fracture strain will be increased by increasing of the aloe vera concentration and changing the other electrospinning parameters (applied voltage, tip/collector distance, feeding rate), this could be associated with the formation of the hydrogen bond between the hydroxyl groups in PVA/AV-PCL scaffolds structure and the decreases of fibers diameter which increases its strength [28,31].

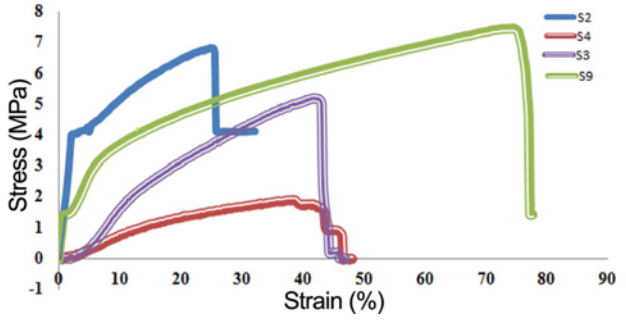

Figure 4. Stress-strain curves of the PVA/AV-PCL nanofibers hybrid.

DSC

Thermogram of the PCL-PVA/AV nanofibers is shown in Figure 5. Two main peaks were detectable. In the first peak, the enthalpy value is about 1017±1.89 mJ, and the melting temperature in this peak is observed in the range of 59±1.29 °C. In the second peak, the calculated enthalpy is 156±1.21 mJ and this the endothermic peak related to crystalline phase melting, which occurs in the range of 201±2.70 °C to 176±3.30 °C with a maximum temperature of 191±3.69 °C. The endothermic peak for PCL nanofibers related to the melting temperature of crystalline phase was detected with a maximum at 62 °C that decreased to 56 °C in PVA-PCL-AV nanofibers. In addition, for pure PVA, glass transition temperature (Tg) was observed at -81 °C that decreased to 76 °C by adding aloe vera, which could be due

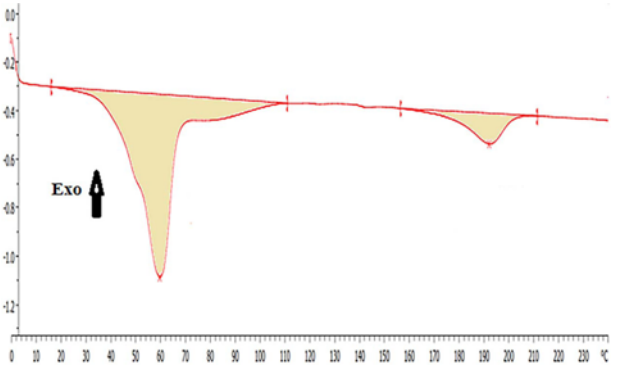

Figure 5. DSC curves PVA/AV-PCL nanofibers.

Table 3. Mechanical properties of the PCL-PVA/AV nanofibers

Scaffold	Elastic modulus (MPa)	Maximum tensile strength (MPa)	Tensile strain (%)
AV: 1 mg/m*l*, V: 18 kV, D: 15 cm, F: 2 m*l*.h^{-1}	1.86±0.57	6.82±1.87	24.79±9.38
AV: 1 mg/m*l*, V: 24 kV, D: 20 cm, F: 3 m*l*.h^{-1}	0.215±0.5	5.19±1.58	41.87±13.42
AV: 4 mg/m*l*, V: 24 kV, D: 15 cm, F: 1 m*l*.h^{-1}	0.08±0.61	1.90±0.70	38.33±14
AV: 6 mg/m*l*, V: 12 kV, D: 15 cm, F: 3 m*l*.h^{-1}	2.02±0.95	8.97±2.16	74.58±22.79

to the presence of aloin in the aloe vera structure [47]. Colbuck *et al.* proved that for pure PCL, the endothermic peak was linked the crystalline phase melting occurring in the range of 30-70 °C with a maximum temperature of 59 °C [48]. Furthermore, according to Nindo *et al.* the melting point of polyvinyl alcohol decreased from 226 °C to 222 °C by the addition of aloe vera. Aloin is a polysaccharide component of the aloe vera structure, which could be completely dissolved in the PVA matrix upon combination with that would significantly affect the crystalline and amorphous structure of the polymer [49,50]. DSC analysis conducted by Zarekhalili *et al.* showed that the pure polycaprolactone melting point was 62 °C, which it was reduced to 56 °C in PVA/GA-PCL scaffold [31]. The DSC thermogram result for PVA/AV-PCL nanofibrous indicated that the hybrid of these nanofibers did not affect their thermal behavior significantly.

Hydrophilicity of Nanofibers

The scaffolds hydrophilicity and hydrophobicity were evaluated through contact angle measurement. Figure 6 shows that PCL/PVA/AV nanofibers are highly hydrophilic. PCL is a hydrophobic semi-crystalline polymer [51]. Unlike PCL, PVA and aloe vera are hydrophilic [44,52]. Based on the studies, PCL contact angle was reported 124 °. Due to contact angle larger than 90 degree, PCL alone cannot be a proper replacement for the injured tissue [53]. Presence of amine and carboxylic groups in the scaffold will enhance its hydrophilicity. Regarding the hydrophilicity of PVA and aloe vera, it is expected that their incorporation with PCL will decline the contact angle [31,52]. Table 4 also lists the measured contact angles of the samples.

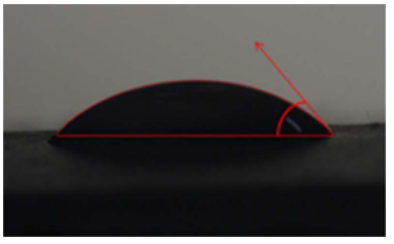

Figure 6. Contact angle measurement of nanofibrous samples.

Table 4. Contact angle measurement of nanofibrous samples

Scaffolds	Contact angle (°)
AV: 1 mg/m*l*, V: 12 kV, D: 10 cm, F: 1 m*l*.h^{-1}	128.22±3.16
AV: 1 mg/m*l*, V: 18 kV, D: 15 cm, F: 2 m*l*.h^{-1}	92.10±1.70
AV: 1 mg/m*l*, V: 24 kV, D: 20 cm, F: 3 m*l*.h^{-1}	76.93±3.30
AV: 4 mg/m*l*, V: 24 kV, D: 15 cm, F: 1 m*l*.h^{-1}	51.22±1.29
AV: 4 mg/m*l*, V: 12 kV, D: 20 cm, F: 2 m*l*.h^{-1}	57.56±2.21
AV: 4 mg/m*l*, V: 18 kV, D: 10 cm, F: 3 m*l*.h^{-1}	64.23±2.62
AV: 6 mg/m*l*, V: 18 kV, D: 20 cm, F: 1 m*l*.h^{-1}	40.19±1.41
AV: 6 mg/m*l*, V: 24 kV, D: 10 cm, F: 2 m*l*.h^{-1}	56.79±0.81
AV: 6 mg/m*l*, V: 12 kV, D: 15 cm, F: 3 m*l*.h^{-1}	39.72±2.62

MTT Assay

Dimethyl thiazole-2 and 5-diphenyl tetrazolium bromide assay was performed to study the viability of L929 fibroblast cells in the PVA/AV-PCL nanofibrous scaffold. Figure 7 showed cells viability on PVA-AV-PCL scaffold, after 3, and 7 days of cell culture. The cell viability for PVA-AV/PCL nanofibers was approximately 106±2.51 % and 114±3.51 % in 3 and 7 days, respectively. The results showed all samples had cell viability of over 80 % and the samples did not show any toxicity. These observations could be associated with the presence of natural polymers AV with exceptional biological feature in the nanofibrous scaffold paving the way for a favorite environment for cell viability of fibroblast cells. Likewise, Jithendra *et al.* [54] argued that proliferation of fibroblast cells on the scaffold containing aloe vera could be associated with the presence of glycoproteins in the aloe vera gel. Therefore, natural polymers increase the proliferation and expression of the fibroblast cell by enhancing the of protein absorption and hydrophilicity nature and of the nanofibrous scaffold [24,55].

Cell Growth and Prolifration

Figure 8 displays the SEM images of L929 fibroblast growth on the scaffolds. SEM images showed good cell proliferation on the scaffolds in a way that numerous colonies were observable by passing of time. In a study by Soganya *et al.*, the presence of glycoprotein in the aloe vera structure was recognized as the major factor in cellular proliferation, growth, and migration in the PCL-AV10 % polymeric scaffold. In fact, the hydrophilic nature of this scaffold due to the presence of aloe vera is one of the reasons for the cellular adhesion and proliferation of fibroblast cells. In addition, the presence of PVA in the scaffold structure provided a favorable condition for the proliferation of

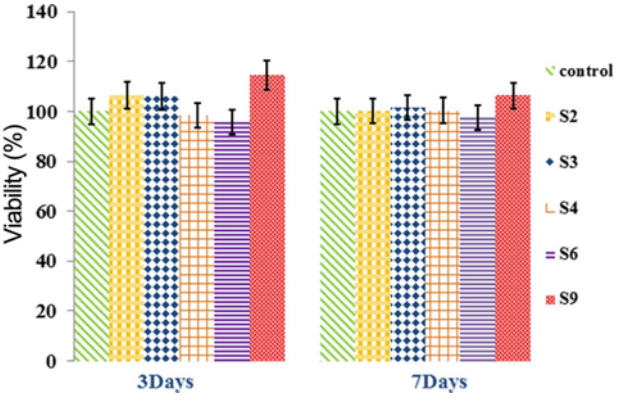

Figure 7. MTT assay of the cell viability for PCL-PVA/AV nanofiber scaffold.

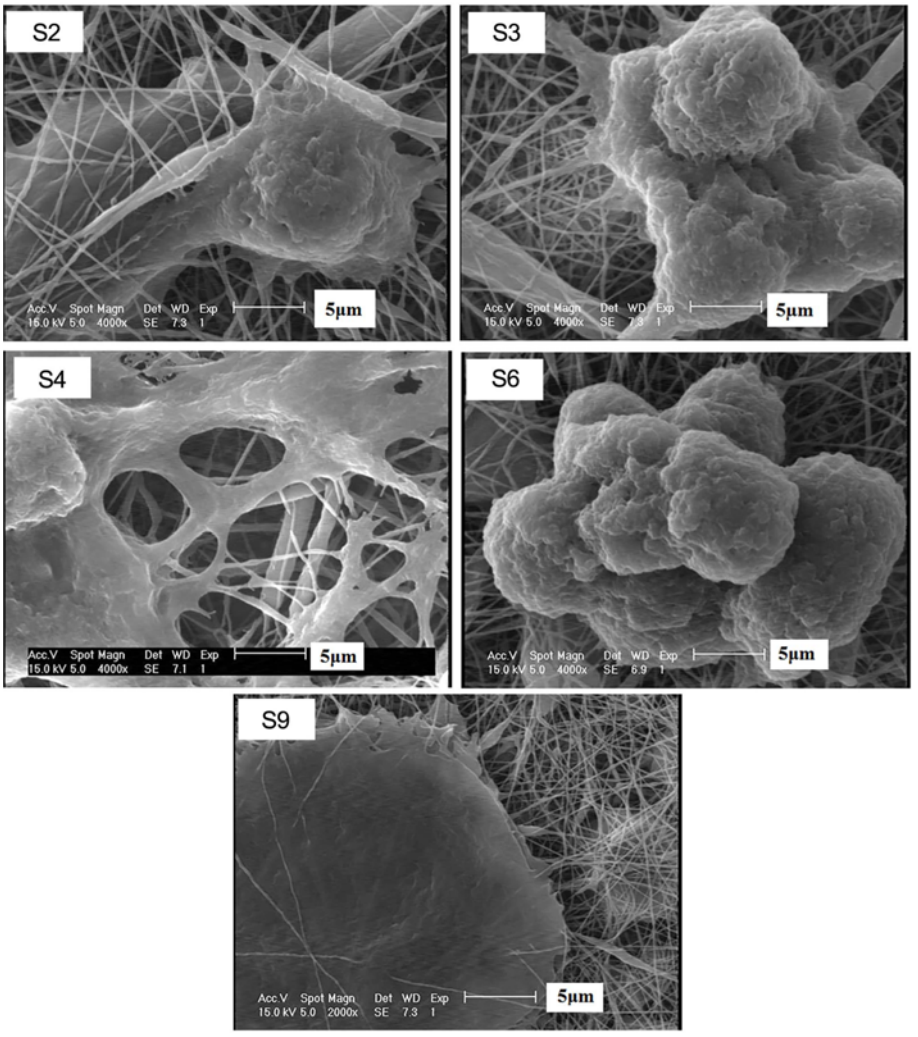

Figure 8. SEM micrograph of cells growth of PVA-AV-PCL nanofiber scaffolds.

fibroblastic cells due to its amino carboxylic functional groups and distinctive biological characteristics. On the other hand, the presence of hydrophilic AV and polyvinyl alcohol along with the hydrophobic polycaprolactone improved the hydrophilicity of the nanofiber facilitating the initial cell bonding on the nanofiber surface, hence, providing the platform for cellular migration, growth and proliferation on the nanofibers [26,44].

As shown in Figure 8, fibroblast cells well bonded to the fibers of all the specimens. There are two fundamental points in these images: in the first and second scaffolds with less aloe vera contents and different electrospinning conditions, the fibroblast cells were attached to the scaffold but they were not expanded on them. In fact, the cells were not sufficiently grown. However, gradual change of the electrospinning parameters and increase of the aloe vera concentration enhanced the cell growth.

Conclusion

In the current study, the electrospinning method was implemented for successful preparation of nanofibrous scaffolds containing PCL-PVA/AV. Taguchi algorithm was applied to explore the influence of electrospinning parameters on the diameter of nanofibers. The results showed that the average diameter of nanofibers decrease with increasing feed rate and voltage. The tip collector distance can increase or decrease the nanofibers diameter. Increasing aloe vera concentration resulted in reduced nanofibers diameter. Nanofibers with the diameter of 119±11.78 nm were chosen as optimum scaffolds. According to the results, the optimum features such as uniform diameter of nanofibers and ideal biological and mechanical characteristics were determined using AV concentration of 6 mg/m*l*, tip/collector distance of 15 cm, applied voltage of 12 kV and flow rate of 3 m*l*/h.

Contact angle tests showed that the PCL-PVA/AV scaffolds have hydrophilic properties. The results of cell culture showed that PCL-PVA/AV scaffolds exhibited excellent cell viability of over 80 % that promoted the cells proliferation. This study sheds light on tailoring nanofibrous scaffold hydrophilicity to enhance proliferation and adhesion of cells for damaged skin reconstruction applications.

References

1. L. Yildirimer, N. T. Thanh, and A. M. Seifalian, *Biotechnology*, **30**, 638 (2012).
2. B. L. Seal, T. C. Otero, and A. Panitch, *Mater. Sci. Eng.*, **34**, 147 (2001).
3. B. Singh, N. Panda, and K. Pramanik, *Macromolecules*, **87**, 201 (2016).
4. A. Baji, Y. W. Mai, and S. C. Wong, *Compos. Sci. Technol.*, **70**, 703 (2010).
5. W. J. Li, R. L. Mauck, and R. S. Tuan, *Biomed. Nanotechnol.*, **1**, 259 (2005).
6. J. M. Deitzel, J. Kleinmeyer, D. E. A. Harris, and N. B. Tan, *Polymer*, **42**, 261 (2001).
7. A. Sonseca, L. Peponi, O. Sahuquillo, J. M. Kenny, and E. Gimenez, *Polym. Degrad. Stabil.*, **97**, 2052 (2012).
8. A. Karchin, F. I. Simonovsky, B. D. Ratner, and J. E. Sanders, *Acta Biomaterialia*, **7**, 3277 (2011).
9. C. L. Casper, J. S. Stephens, N. G. Tassi, D. B. Chase, and J. F. Rabolt, *Macromolecules*, **37**, 573 (2004).
10. S. Megelski, J. S. Stephens, D. B. Chase, and J. F. Rabolt, *Macromolecules*, **35**, 8456 (2002).
11. K. L. Ou, C. S. Chen, L. H. Lin, J. C. Lu, Y. C. Shu, W. C. Tseng, J. C. Yang, S. Y. Lee, and C. C. Chen, *Eur. Polym. J.*, **47**, 882 (2011).
12. F. Roozbahani, N. Sultana, A. F. Ismail, and H. Nouparvar, *Nanomaterials*, **2013**, 641502 (2013).
13. J. Doshi and D. H. Reneker, *Electrostatics*, **35**, 151 (1995).
14. E. J. Chong, T. T. Phan, I. J. Lim, Y. Z. Zhang, B. H. Bay, S. Ramakrishna, and C. T. Lim, *Acta Biomaterialia*, **3**, 321 (2007).
15. G. Ma, D. Fang, Y. Liu, X. Zhu, and J. Nie, *Carbohydr. Polym.*, **87**, 737 (2012).
16. T. T. T. Nguyen, O. H. Chung, and J. S. Park, *Carbohydr. Polym.*, **86**, 1799 (2011).
17. H. Lonnberg, K. Larsson, T. Lindstrom, A. Hult, and E. Malmstrom, *ACS Appl. Mater. Interfaces*, **38**, 3484 (2009).
18. S. U. Maheshwari, S. V. Kumar, N. Nagiah, and T. S. Uma, *Polym. Bull.*, **70**, 2995 (2013).
19. J. H. Hamman, *Molecules*, **13**, 1599 (2008).
20. K. Eshun and Q. He, *Critical Reviews in Food Science and Nutrition*, **44**, 91 (2004).
21. R. Maenthaisong, N. Chaiyakunapruk, S. Niruntraporn, and C. Kongkaew, *Burns*, **33**, 713 (2007).
22. J. M. A. Antonisamy, N. Beaulah, R. Laju, and G. Anupriya, *Biomed. Adv. Res.*, **3**, 184 (2012).
23. I. Garcia-Orue, G. Gainza, F. B. Gutierrez, J. J. Aquirre, J. L. Pedraz, and M. Lgartua, *Pharmaceutics*, **523**, 556 (2017).
24. S. Suganya, J. Venugopal, S. Ramakrishna, B. S. Lakshmi, and V. G. Dev, *Biol. Macromol.*, **68**, 135 (2014).
25. S. S. Silva, E. G. Popa, M. E. Gomes, M. Cerqueira, A. P. Marques, S. G. Caridade, P. Teixeira, C. Sousa, J. F. Mano, and R. L. Reis, *Acta Biomaterialia*, **9**, 6790 (2013).
26. N. A. Abdullah, K. A. Sekak, M. R. Ahmad, and T. B. Effendi, "Proceedings of the International Colloquium in Textile Engineering", Fashion, Apparel and Design, 2014.
27. F. R. Isfahani, H. Tavanai, and M. Morshed, *Fiber. Polym.*, **18**, 264 (2017).
28. P. Carter, S. M. Rahman, and N. Bhattarai, *J. Biomater. Sci.*, **27**, 692 (2016).
29. Z. Thompson, S. Rahman, S. Yarmolenko, J. Sankar, D. Kumear, and N. Bhattarai, *Materials*, **10**, 937 (2017).
30. S, Baghersad, S. H. Bahrami, M. R. Mohammadi, M. R. M. Mojtahedi, and P. B. Milan, *Mater. Sci. Eng.*, **93**, 367 (2018).
31. Z. Zarekhalili, S. H. Bahrami, M. Ranjbar Mohammadi, and P. B. Milan, *Int. J. Biol. Macromol.*, **94**, 679 (2017).
32. N. Bhardwaj and S. C. Kundu, *Biotechnol. Adv.*, **28**, 325 (2010).
33. P. Vashisth, P. A. Pruthi, R. P. Singh, and V. Pruthi, *Carbohydr. Polym.*, **109**, 16 (2014).
34. G. Kalita, S. Adhikari, H. R. Aryal, P. R. Somani, S. P. Somani, M. Sharon, and M. Umeno, *Diamond and Related Materials*, **17**, 799 (2008).
35. D. K. Ki, D. N. Han, and H. T. Kim, *Chem. Eng.*, **104**, 55 (2004).
36. D. C. Montgomery, "Design and Analysis of Experiments", Wiley and Sons, 2017.
37. S. Michael, G. Ermanno, P. Marion, and G. Julia, *Nature*, **327**, 239 (1987).
38. A. Salati, H. Keshvari, H. G. Ahangari, and M. H. Sanati, *Biointerface Res. Appl. Chem.*, **6**, 1214 (2016).
39. M. P. Mani and S. K. Jaganathan, *J. Text. Inst.*, **110**, 1615 (2019).
40. H. S. Mansur, C. M. Sadahira, A. N. Souza, and A. A. Mansur, *Mater. Sci. Eng.*, **28**, 539 (2008).
41. J. Ranjana and N. Sharma, *Macromolecules*, **94**, 679 (2017).
42. S. C. Baker, N. Atkin, P. A. Gunning, N. Granville, K. Wilson, D. Wilson, and J. Southgate, *Biomaterials*, **27**, 3136 (2006).
43. L. Tan, J. Hu, H. Huang, J. Han, and H. Hu, *Biol. Macromol.*, **79**, 469 (2015).
44. S. Suganya, J. Venugopal, S. A. Mary, S. Ramakrishna, B. S. Lakshmi, and V. G. Dev, *Iranian Polymer*, **23**, 237 (2014).
45. M. P. Mani and S. K. Jaganathan, *J. Ind. Text.*, 152808371984062 (2019).
46. M. P. Mani, S. K. Jaganathan, P. Prabhakaran, E. Supriyanto, and A. F. Ismail, *Int. J. Polym. Anal. Characterization*, **24**, 457 (2019).

47. J. W. Sahayraj, C. Kumar, S. Rajendran, S. K. Selvaraj, A. P. P. Regis, and R. Mohan, *Eur. Chem. Bull.*, **2**, 315 (2013).
48. D. Kolbuk, P. Sajkiewicz, K. Maniura-Weber, and G. Fortunato, *Eur. Polym. J.*, **49**, 2052 (2013).
49. C. I. Nindo, J. R. Powers, and J. Tang, *Trans. ASABE*, **53**, 1193 (2010).
50. H. Chen, J. Honglin, J. Yu, S. Liu, and P. Gu, *Biol. Macromol.*, **48**, 13 (2011).
51. P. Nugroho, H. Mitomo, F. Yoshi, T. Kume, and K. Nishimura, *Macromol. Mater. Eng.*, **286**, 316 (2001).
52. S. R. Gomes, G. Rodrigues, G. G. Martins, M. A. Roberto, M. Mafra, and C. M. R. Henriques, *Mater. Sci. Eng.*, **46**, 348 (2015).
53. M. Kharaziha, M. H. Fathi, and H. Edris, *Sci. Technol.*, **87**, 182 (2013).
54. P. Jithendra, A. M. Rajam, T. Kalaivani, and A. B. Mandal, *ACS Appl. Mater. Interfaces*, **5**, 7291 (2013).
55. L. Ghasemi-Mobarakeh, M. P. Prabhakaran, M. Morshed, M. H. Nasr-Esfahani, and S. Ramakrishna, *Biomaterials*, **29**, 4532 (2008).